Korean J. Chem. Eng., **21**(2), 404-411 (2004)

Modeling Percolative Fragmentation during Conversion of Entrained Char Particles

Francesco Miccio†

Istituto Ricerche sulla Combustione - CNR, via Metastasio 17, 80125 Napoli, Italy
(*Received 9 May 2003 • accepted 6 October 2003*)

Abstract−A numerical model of carbonaceous particle conversion under chemical and external diffusion control is proposed. The model accounts for different classes of particles which undergo chemical conversion in parallel with percolative fragmentation. It applies to typical conditions of entrained flow reactors. The system of algebraic and differential equations has been numerically solved. Results include the total carbon conversion as well as the determination of particle properties along the reactor. The model correctly predicts the change of the conversion rate at varying temperature, initial oxidant concentration and excess oxidant ratio. The influence of percolation parameters is also relevant and claims further investigations for more accurate determination. A comparison with experimental data available in literature is also provided.

Key words: Percolation, Char, Combustion, Gasification, Carbon Conversion

INTRODUCTION

Comminution phenomena include fragmentation and attrition mechanisms, leading to the breaking of a mother fuel particle, its size reduction and the consequent generation of smaller fragments [Chirone et al., 1991]. Among these phenomena, percolative fragmentation is responsible for carbon depart emission as fine particles from chars in the course of chemical conversion upon the vanishing of structural links between parts of the solid particle [Kerstein and Niksa, 1984]. The extent and the topological properties of internal particle porosity largely influence the course and the role played by percolation. The characteristic size of percolated fragments is in the range 0.1-100 μm [Kang et al., 1988; Salatino and Massimilla, 1988] and is related to the extent of the internal char macro-porosity. Nevertheless, the relative formation rate of percolated fragments as well as their size distribution largely depends also on the particle conversion regime [Chirone et al., 1991]. Conversion of percolated fragments can be inhibited if they quickly escape the reactor chamber (e.g., bubbling fluidized or fixed beds) as a consequence of an inadequate reactor size or residence time. Therefore, process efficiency, apparent kinetics, burn-off time and conversion degree could be significantly affected by occurrence of percolative fragmentation. From a practical point of view, percolative fragmentation can be responsible for fly-ash emissions in addition to attrition-generated particulates or to fines contained in the in the fuel feed-stock [Jung and Park, 1988].

Experimental studies on percolative fragmentation during combustion/gasification have been proposed by a number of investigators [Kerstein and Edwards, 1987; Kang et al., 1988; Salatino and Massimilla, 1988; Mitchell and Jacob Akatenuk, 1996; Liu et al., 2000]. In addition, models based on both continuous and discrete approaches have been developed and applied to predict the percolation behavior of porous carbon particles [Kerstein and Niksa, 1984; Sahimi and Totsis, 1987; Kang et al., 1988; Miccio and Salatino, 1992; Salatino et al., 1993; Fuertes and Marban, 1994; Mitchell and Jacob Akatenuk, 1996; Liu et al., 2000]. In particular, Salatino et al. [1993] proposed a particle conversion model for carbon gasification, which includes the effect of percolation, evaluated on the basis of a discrete model by Miccio and Salatino [1992]. Their approach allows the determination of the impact of percolation on conversion efficiency, when generated fragments are free to leave the reactor. Fuertes and Marban [1994] presented a model of gasification of a single porous particle taking into account percolative fragmentation. They demonstrated that the conversion time is largely influenced by structural particle properties and the onset of percolation.

The relevance of percolation in a real system has been recently addressed by Miccio et al. [1999], who extensively investigated the generation rate of fine particles issuing from a fluidized bed gasifier fed with a biomass fuel. They reported that the fluidized bed is unable to completely convert fixed carbon and, consequently, the elutriation rate dramatically increases under less favorable conditions of gasification. The experimental measurements of carbon concentration at different reactor elevations also confirmed that percolative fragmentation occurs during the passage in the freeboard as a consequence of chemical conversion.

The present paper proposes a new numerical model of carbonaceous particle conversion (combustion or gasification) in entrained flow. Different from models available in literature [Kerstein and Niksa, 1984; Sahimi and Totsis, 1987; Kang et al., 1988; Miccio and Salatino, 1992; Salatino et al., 1993; Fuertes and Marban, 1994; Mitchell and Jacob Akatenuk, 1996; Liu et al., 2000] that are mainly focused on the evolution of a single char particle, the whole reactor (combustor or gasifier) is here considered. The study is an attempt at combining equations of mass balance, population balance, mass transfer, chemical kinetics and percolation rate to predict the evolution of char particles and the overall conversion degree in the reactor. The model accounts for different sizes of char particles undergoing chemical conversion in parallel with percolative fragmentation. The role played by percolative fragmentation is analyzed and discussed with reference to a base case of model input variables. A

†To whom correspondence should be addressed.
E-mail: miccio@irc.na.cnr.it

comparison between model results and experimental data taken from Miccio et al. [1999] is also provided.

MODEL DESCRIPTION

A vertical entrained flow reactor is considered. Char particles are continuously fed at the bottom of the tube and entrained by a gas stream containing an oxidant species and flowing upward. Following assumptions are made.

1. Model Assumptions

(1) Char particles are spherical.

(2) Plug flow is assumed for the gas stream. The gas velocity is not affected by solid particles.

(3) Gas and particles have the same constant temperature.

(4) Chemical conversion of particles occurs under the kinetically controlled regime with a shrinking core mechanism. Intra-particle resistance to diffusion is neglected.

(5) No attrition phenomena occur. Upon particle conversion, fuel ashes form a coherent skeleton.

(6) The dependence of the surface area on the conversion degree of particles is known.

(7) Percolative fragmentation takes place in parallel with chemical conversion. The relative percolation rate depends on particle voidage, until a percolation voidage threshold is reached, after that the particle collapses.

(8) Fragments formed by percolative fragmentation have a known size.

It is worth noting that assumption 4 applies reasonably well to the case of entrained conversion of chars at intermediate temperatures (up to 1,200 K). Assumption 6 is needed because the surface area, and consequently the char apparent kinetics, changes as the conversion degree and particle voidage increase.

2. Model Equations

Particle size distribution is accounted for by introducing a finite number of particle classes with nominal size d. For each class the initial mass fraction is assigned. The same values of initial voidage, surface area and carbon content are adopted for each class.

Eq. (1) accounts for the mass balance for i-th particle class. Generation terms by both chemical conversion and percolative fragmentation ($G_{chem,i}$ and $G_{perc,i}$) are considered. $P_{j,i}$ represents the fraction of fragments percolated from other class $j \neq i$ with size d_i.

$$\frac{1}{S}\frac{d}{dz}w_i = G_{chem,i} + G_{perc,i} - \sum_j (G_{perc,j} P_{j,i}) \tag{1}$$

Eq. (2), which accounts for the ash conservation, is directly derived from the previous equation by introducing the carbon content x_i.

$$\frac{1}{S}\frac{d}{dz}w_i(1-x_i) = G_{perc,i}(1-x_i) - \sum_j G_{perc,j} P_{j,i}(1-x_j) \tag{2}$$

The momentum conservation for particles of class i is reported in Eq. (3), where the acceleration term equals the sum of drag force, gravity and momentum of percolated fragments.

$$\frac{d}{dz}w_i u_i = \pi \frac{n_i}{u_i}\left(3\mu d_i |U-u_i|\left(1+\frac{3}{8}\frac{\rho_g |U-u_i| d_i}{\mu}\right) - \frac{d_i^3 \rho_i}{6}(1-\varepsilon_i)g\right) + S[G_{perc,j} u_j - \sum_j (G_{perc,j} P_{j,i} u_j)] \tag{3}$$

The population balance over particles of class i is provided by Eq. (4), in which the derivative of particle frequency is equated to the summation of percolation rates, giving the generation rate of new particles.

$$\frac{1}{S}\frac{d}{dz}n_i = -\frac{1}{\frac{\pi}{6}d_i^3}\sum_j \frac{G_{perc,j} P_{j,i}}{(1-\varepsilon_j)\rho_j} \tag{4}$$

The generation by chemical conversion is calculated via Eq. (5); it depends on the oxidant molar fraction $Y_{s,i}$, the surface area A_i, the surface kinetic constant k and the fraction of surface ξ occupied by carbon sites.

$$G_{chem,i} = -\frac{\pi}{6S} d_i^3 A_i \frac{n_i}{u_i} k e^{-\frac{E_{act}}{R_g T}} Y_{s,i}^{\gamma} \xi_i \tag{5}$$

The generation by percolative fragmentation is related to chemical conversion via Eq. (6), by introducing the dimensionless percolative fragmentation rate R_i [Miccio and Salatino, 1992]

$$G_{perc,i} = G_{chem,i} \frac{R_i}{1-R_i} \tag{6}$$

Fine fragments generated from coarse particles have the characteristic size of the smaller class of particles, irrespective of the particle class from which they originate.

The mass transfer between gas and particles external surface is expressed by Eq. (7) under the hypothesis of steady state condition.

$$\pi d_i^2 n_i h_m (Y - Y_{s,i}) \frac{P}{R_g T} = -S \frac{G_{chem,i}}{0.012} u_i \tag{7}$$

where the coefficient of mass transport h_m is evaluated by Eq. (8).

$$h_m = \frac{DT^{\lambda}\frac{101325}{P}}{d_i}\left[2 + 0.6\left(\frac{\rho\mu}{DT^{\lambda}\frac{101325}{P}}\right)^{1/3}\left(\frac{\rho|U_g - u_i| d_i}{\mu}\right)^{1/2}\right] \tag{8}$$

The particle voidage ε_i and the average particle density ρ_i are calculated via Eqs. (9) and (10), respectively.

$$\varepsilon_i = 1 - \frac{w_i}{n_i \frac{\pi}{6} d_i^3 \rho_i} \tag{9}$$

$$\rho_i = \left(\frac{x_i}{\rho_c} + \frac{1-x_i}{\rho_a}\right)^{-1} \tag{10}$$

The surface area A_i is calculated by Eq. (11) following Bathia and Perlmutter [1980]. It is a function of the initial area A_0, the initial and current particle voidage (ε_0, ε_i) and the parameter Ψ, which depends on the char morphology.

$$A_i = A_0\left(\frac{1-\varepsilon_i}{1-\varepsilon_0}\right)\left[1 - \Psi \ln\left(\frac{1-\varepsilon_i}{1-\varepsilon_0}\right)\right]^{1/2} \tag{11}$$

The fraction of the surface area covered by carbon is expressed by Eq. (12) and depends on the carbon content only.

$$\xi_i = \frac{x_i}{\rho_c}\left(\frac{x_i}{\rho_c} + \frac{1-x_i}{\rho_a}\right)^{-1} \tag{12}$$

The current concentration of the oxidant species Y and the total car-

bon conversion degree χ are given by Eqs. (13) and (14), respectively.

$$Y = Y_o - \frac{\sum_i (w_{o,i}x_{o,i} - w_i x_i)}{0.012}\frac{RT}{SUP} \quad (13)$$

$$\chi = 1 - \frac{\sum_i w_i x_i}{\sum_i w_{o,i}x_{o,i}} \quad (14)$$

The dimensionless percolation rate is expressed by Eq. (15), which takes into account both peripheral and uniform percolation. Percolation rate is proportional to the chemical rate in the earlier stage of conversion and diverges (i.e., particle disintegration) when internal voidage approaches the percolative threshold ε_{cr}.

$$R_i = \frac{R_0}{(\varepsilon_{cr} - \varepsilon)^{\nu}} \quad (15)$$

3. Initial Conditions

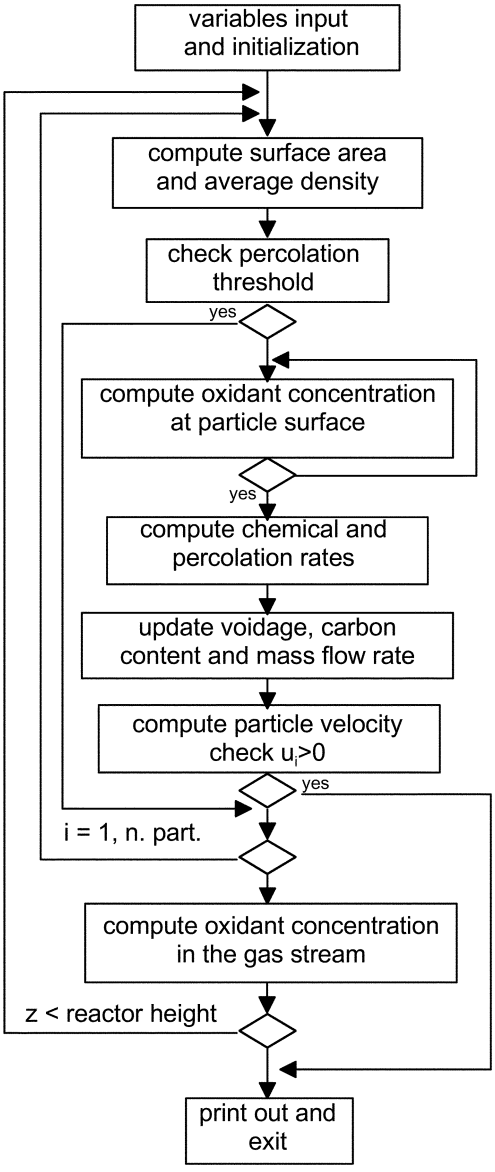

Fig. 1. Flow-chart of the numerical procedure adopted for the model implementation.

The initial conditions (see Eqs. (16), (17) and (18)) are imposed at z=0 on mass flow rate, particle velocity and particle frequency.

$$w_i = w_{i,o} = \frac{0.012}{x_0}\frac{SUP}{RT}\frac{Y_g}{e}\Phi_{i,0} \quad (16)$$

$$u_i = 0 \quad (17)$$

$$n_i = \frac{w_{i,0}}{\frac{\Pi}{6}d_i^3}\frac{\frac{x_0}{\rho_c} + \frac{1-x_0}{\rho_a}}{1-\varepsilon_0} \quad (18)$$

4. Computing

The system of algebraic and differential equations has been numerically solved by means of an explicit algorithm of integration after discretization over a fixed spatial 1-D grid. A flow chart of the whole numerical procedure is shown in Fig. 1. The computation of the oxidant concentration at external particle surface, via Eq. (7), requires an iterative procedure. Calculations have been executed on a Pentium™ IV personal computer running Visual Fortran™ 5.0. Results of a single run include the profile along z coordinate of variables x, w, Y_s and ε for each particle class, as well as the profiles of total carbon conversion (χ) and oxidant molar fraction (Y).

RESULTS AND DISCUSSION

1. Base Case Results

A base case for calculations has been selected by adopting values of input model variables reported in Table 1. A mixture of particles with two characteristic sizes (bi-modal) is considered for simplicity, the larger size being dominant in the mass distribution (90%). Percolated fragments have a size of 10 μm, which is of the same order of magnitude as macro-porosity for biomass chars. Percolation rate is assumed at values indicated by Miccio and Salatino [1992] for 3-D porous lattices under chemically controlled conversion regime, whose condition maximizes the impact of percolative fragmentation. Percolation threshold was set at the value 0.8, which is in the range of experimental data furnished by Kerstein and Niksa [1984]. Kinetic data are chosen in the typical range of biomass chars for combustion in air [Senneca et al., 2002].

Fig. 2 shows the evolution of the carbon conversion degree and oxidant molar fraction along the reactor axis (base case). It appears that the carbon conversion rate is initially fast thanks to the presence of small char particles (i.e., d=10 μm) in the fuel stream. In the intermediate section of the reactor the slope of the conversion curve is lowered, the small particles being completely converted. At the reactor coordinate 1.6 m a sharp increase of the reaction rate is noted, as a consequence of coarse particles collapsing upon attainment of the percolation threshold. New generated fines quickly react and the carbon conversion is completed at approximately 2.2 m. Of course, results concerning carbon conversion are also reflected in the oxidant concentration curve. In the same figure, curves obtained in absence of percolation (i.e., R_0=0 and ε_{cr}=1.0) are also plotted for comparison. It clearly appears that carbon conversion is dramatically affected and the reactor is inadequate to reach total carbon conversion.

Fig. 3 shows the evolution of the voidage (Fig. 3A) and the carbon content (Fig. 3B) along the reactor for different particle classes.

Table 1. Values of input model variables

	Base case		Exp. comparison	
Carbon content (x_0)	0.8		0.56	
Number of particle classes	2		2	
	Size (d_i), μm	Mass fraction ($\Phi_{i,0}$)	Size (d_i), μm	Mass fraction ($\Phi_{i,0}$)
Particle class #1	10	0.1	10	0.29
Particle class #2	120	0.9	200	0.71
Particle voidage (ε_0)	0.6		0.8	
Percolation threshold (ε_{cr})	0.8		0.9	
Percolation rate (R_0)	0.15		0.2	
Percolation exponent (ν)	0.2		0.2	
Size of percolated fragments, μm	10		10	
Surface area (A_0), m^{-1}	6×10^6		6×10^6	
Bhatia & Perlmutter coefficient (Ψ)	10		10	
Carbon density (ρ_c), kg m^{-3}	2200		2200	
Ash density (ρ_a), kg m^{-3}	1800		1800	
Temperature (T), K	1300		1100	
Pressure (P), Pa	101325		101325	
Excess of the oxidant species (e)	1.1		1.4	
Gas velocity (U), m s^{-1}	2.0		0.4	
Reactor section (S), m^2	1.0		0.0142	
Reactor height (L), m	3.0		1.8	
Pre-exp. factor (k), kg m^{-2} s^{-1}	2.5×10^4		5.0×10^4	
Activation energy (E_{act}), J mol^{-1}	1.5×10^5		2.0×10^5	
Reaction order (γ)	1.0		0.6	
Molar fraction of the oxidant (Y_0)	0.21		0.18	
Gas diffusion (D), m^2 s^{-1}	$1.\ 10^{-10}$		$1.\ 10^{-10}$	
Gas diffusion exponent (λ)	1.75		1.75	

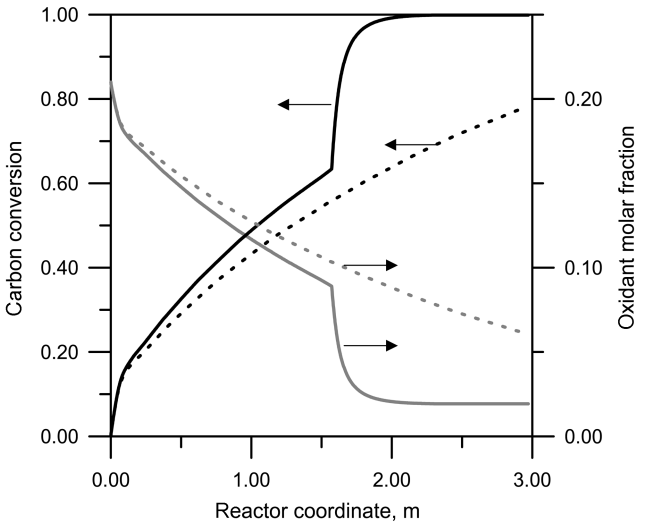

Fig. 2. Carbon conversion degree and oxidant molar fraction versus reactor coordinate (solid lines=base case, dotted lines= no percolation).

A sharp decay of carbon content can be noted for the small class (d=10 μm), whose originally charged particles disappear only within 0.15 m. In the range of the reactor coordinate 0.15-1.6 m, the continuous generation of fine particles from coarse ones can be noted, the curve of carbon content (d=10 μm) attaining a small positive and roughly constant value. Coarse particles have a slower conversion rate as a consequence of the increased external resistance to the mass transfer. They collapse at z=1.6 m when particle voidage equals ε_{cr} (Fig. 3A), leading to the generation of a large number of fines. Correspondingly, a peak appears in the curve of carbon content for fine particles (Fig. 3B), as a consequence of coarse particle disintegration. The percolated fines are once again quickly converted in the final zone of the reactor. It is worth noting that in a real case the presence of multiple or continuous size distribution of particles, as well as a non uniform percolation behavior of chars, is expected to sensibly smooth the peak.

The evolution of the oxidant molar fraction Y_s at the particle surface is presented in Fig. 4 for both fine and coarse particles. The gas bulk concentration is also plotted for comparison. A different behavior between the two particle classes clearly appears in the figure. In fact, a gap between the curve Y_s for fines and that of gas bulk concentration can be noted at the reactor inlet only, when the conversion rate reaches very high values. In the remaining section, curves for fines and gas bulk overlap. On the contrary, Y_s attains a very low value for coarse particles. An explanation for these results can be found in the inverse dependence of the mass transfer coefficient on particle diameter (see Eqs. (7) and (8)). Coarse particles have a relatively low mass transfer rate from gas to the external surface and the available oxidant at the surface is almost completely de-

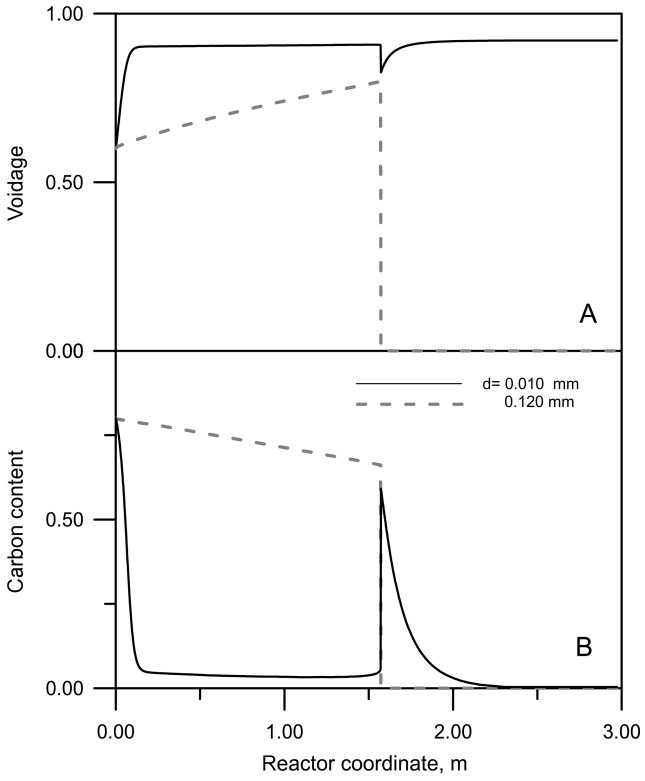

Fig. 3. Voidage (A) and carbon content (B) for two particle classes versus reactor coordinate (base case).

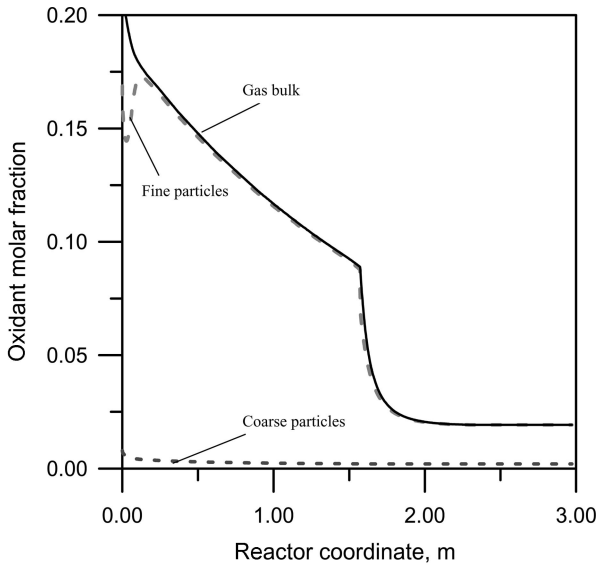

Fig. 4. Oxidant molar fraction at particle surface for coarse and fine particles and in bulk gas versus reactor coordinate (base case).

pleted by the occurrence of chemical reaction in the porous network. Therefore, the external resistance to mass transfer has a larger role for coarse particles, depressing Y_s, and becomes negligible for small particles. This limiting effect is reflected in the lower conversion rate shown by coarse particles in comparison to fine ones, until percolation threshold is reached (see Fig. 3).

2. Role Played by Model Variables

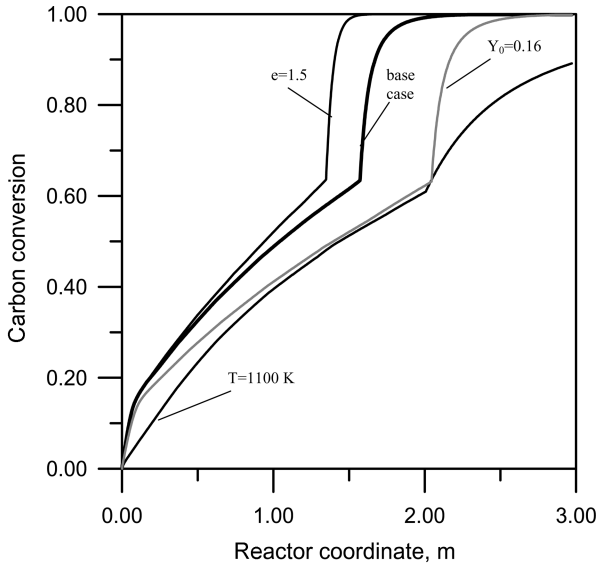

Fig. 5. Carbon conversion versus reactor coordinate for different values of model input variables (base case, e=1.5, Y_0=0.16 and T=1,100 K).

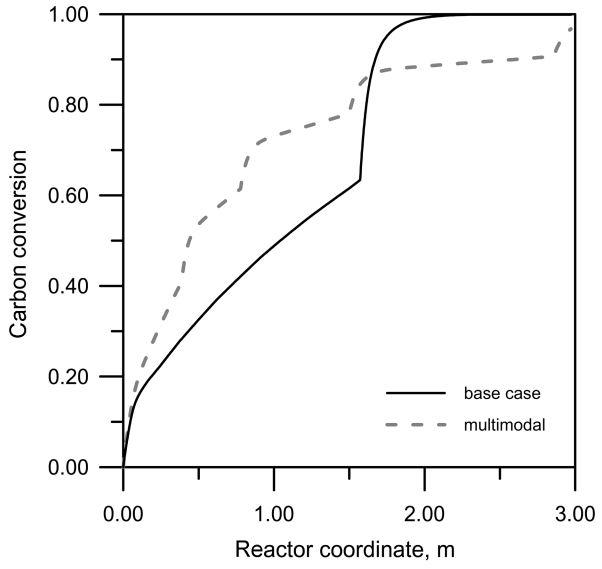

Fig. 6. Carbon conversion versus reactor coordinate for bi-modal (base case) and multi-modal particle distribution (d=10, 60, 80, 100, 120 μm).

Fig. 5 reports profiles of carbon conversion obtained changing each one of the following at a time with respect to the base case: i) the oxidant excess, ii) the reactor temperature, and iii) the initial oxidant concentration. The model correctly predicts the decrease of the conversion rate when temperature or oxidant concentration is lowered. In such cases the coarse particle disintegration occurs in the final zone of the reactor and, consequently, the residence time of percolated fines is insufficient in order to achieve complete carbon conversion. The increase of the oxidant excess enhances the chemical conversion rate and, in turn, percolation rate, leading to a left-shifted curve with respect to the base case.

Fig. 6 compares the profile of carbon conversion for base case

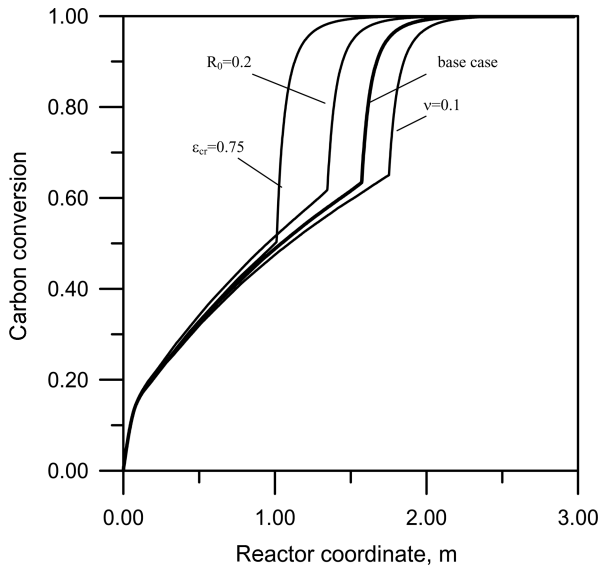

Fig. 7. Carbon conversion versus reactor coordinate for different values of percolation parameters (base case, R=0.25, ε_{cr}= 0.75, ν=0.1).

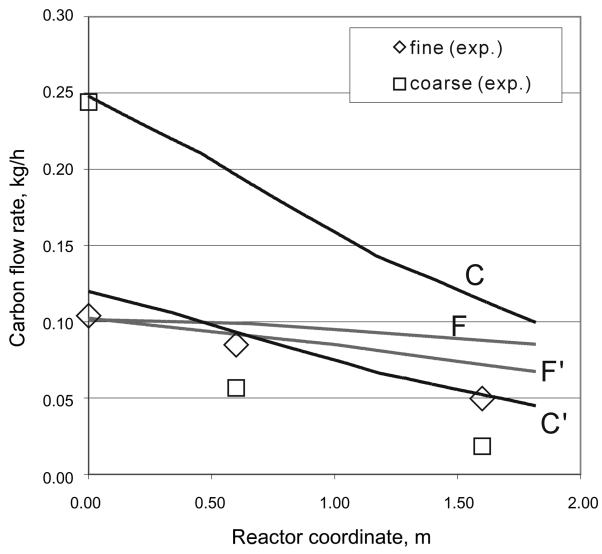

Fig. 8. Carbon flow rate versus reactor coordinate: comparison between experimental (symbols) and model results (lines).

(bi-modal) with that calculated when a mixture based on five particle sizes (multi-modal) is fed to the reactor. A number of steps clearly appear in the latter curve, corresponding to collapse events by the percolation of each particle class in the multi-modal distribution. As a consequence, carbon conversion occurs more gradually along the reactor. It is worth noting that for multi-modal particle distribution the reactor length is insufficient to achieve full conversion, even if the top particle size is the same in both bi-modal and multi-modal distribution (i.e., 120 μm). This apparent paradox can be explained by considering the increased generation rate of fine particles in the initial section of the reactor induced by multiple fragmentation events. Since fine particulate reacts more quickly, the oxidant concentration is lowered and the conversion rate of coarse particles is depressed with respect to the base case.

Fig. 7 shows the influence of percolation rate parameters (see Eq. (15)) on carbon conversion. Increasing both R_0 and ν leads to the emphasizing of the role of percolation and to the shifting of the curve of carbon conversion to the left. Decreasing the percolation threshold ε_{cr} exerts the principal effect of anticipating coarse particle disintegration. In fact, the curve for ε_{cr}=0.75 practically follows that of base case until z=1.0; after that it departs sharply as a consequence of the anticipated particle collapse. The analysis of the influence exerted by percolation parameters (Eq. (15)) clearly indicates the role played by percolative fragmentation: the easier the generation of percolated fine particles, the higher the apparent kinetics. This finding agrees with conclusions reported by Marban and Fuertes [1997] concerning the reactivity of single particles undergoing percolative fragmentation.

3. Model Validation

The model has been compared and validated against experimental results provided by Miccio et al. [1999] and other unpublished data concerning fluidized bed gasification in air of a biomass fuel (beech wood). Experimental results of carbon post conversion in the freeboard have been used so far. The experiments were carried out in a fluidized bed unit operated at 800 °C and at a global equivalence ratio (volume of stoichiometric air/volume of air) equal to 6.7. Model input variables adopted for the validation are reported in the last column of Table 1. The carbon content is reduced whereas the average size of coarse particle is increased, according to experimental measurements. Carbon dioxide is considered as gasifying agent, at concentration Y_0=0.18 as reported by Miccio et al. [1999]. Activation energy ($E_{act}=2\times10^5$ J mol^{-1}) and reaction order (γ=0.6) are directly taken from data reported by Risnes et al. [2001] for CO_2 gasification of biomass chars. The pre-exponential factor is set to 5×10^4 kg m^{-2} s^{-1}, corresponding to a volume based kinetic rate of 6.8×10^8 s^{-1}. This value is one order of magnitude higher than that reported by Risnes et al., 2001 (2.2×10^7 s^{-1}). Design and operating variables are set to the actual values of the experiments. Measurements of carbon concentration [Miccio et al., 1999] are worked out in order to obtain the excess of the oxidant (e=0.14) and the initial mass fraction of coarse ($\Phi_{i,0}$=0.71) and fine ($\Phi_{i,0}$=0.29) particles escaping fluidized bed and entrained upward in the freeboard. These values are reported in Fig. 8 by using different symbols (squares and diamonds). In the same figure, the results of the present model are also shown as continuous curves C and F for coarse and fine particles, respectively. The initial point of calculation coincides with the first experimental point for both curves, as a trivial consequence of the input variable choice. A monotonic decrease of carbon flow rate with the reactor coordinate is predicted by the model. It appears that the conversion rate is larger for coarse particles (C curve) by virtue of the parallel path of particle conversion by percolation. Anyway, the percolation threshold was not achieved within the total residence time in the reactor. The model overestimates the experimental points in both cases of coarse and fine particles, even if it correctly predicts their decaying trend. Reasons for this low figure could be found in the uncertainties about adopted input variables, as well as in a higher particle temperature. The latter is compensated by the choice of a higher pre-exponential factor with respect to data reported in literature [Risnes et al., 2001]. By virtue of the temperature dependence, the one-order-of-magnitude increase in kinetics could be obtained at a higher particle temperature (around 1,230 K).

A temperature increase of 100-200 K seems to be reasonable for experimental conditions, the particle conversion rate not being fast. As far as experimental data are concerned, Miccio et al. [1999] reported that their measurements of carbon concentration at the lowest reactor elevation (i.e. z=0) were probably overestimated, as a consequence of splashing region phenomena. The experimental error can be principally attributed to coarse particles only, for which inertial effects of the splashing zone are more relevant. Therefore, the model calculations were repeated by halving the initial mass flow rate of coarse particles (curve C' and F' in Fig. 8) leading to a drastic reduction of the gap between experimental and model results. In conclusion, the curves C' and F' in Fig. 8 provide a good fit of experimental data under an arbitrary but reasonable correction of input data, namely, a drastic reduction of the coarse particle content and the increase of 157 K in the particle temperature.

CONCLUSIONS

A numerical model of carbonaceous particle conversion in entrained flow was developed. The model accounts for different classes of char particles that undergo chemical conversion with shrinking core mechanism in parallel to percolative fragmentation.

The model correctly predicts the dependence of the conversion rate on temperature, initial oxidant concentration and oxidant excess. Changes of the apparent conversion rate are not only due to chemical effects but also to the increased external diffusion rate, when small fragments are generated by percolation.

Model results are sensitive to percolation parameters, whose estimation deserves particular care in order to have accurate model predictions. To this aim, further modeling and experimental efforts are recommended.

The comparison of model predictions with experimental results of char conversion and percolation available in literature is overall satisfactory. The choice of the pre-exponential factor or, in other words, the particle temperature, is crucial in order to have a good fit of experimental data. However, the evaluation of particle temperature is out of the scope of this present study. Under conditions examined in the present research (i.e., kinetically controlled regime and shrinking core mechanism of conversion), percolative fragmentation can be considered as an accelerating factor of the conversion rate, and neglecting percolation leads to an over-estimation of global conversion time.

ACKNOWLEDGMENTS

The research has been partly carried out within the framework of a research fellowship sponsored by Alexander Von Humboldt Foundation. Dr. O. Senneca is gratefully acknowledged for helpful discussion on char particle kinetics.

NOMENCLATURE

$A_{0,i}$, A_i : initial, current surface area [m^{-1}]
d_i : nominal size of particle classes [m]
D : gas diffusion coefficient
e : excess of the oxidant species
E_{act} : activation energy [J mol^{-1}]
$F_{i,0}$: initial mass fraction of particles
g : acceleration of gravity [m s^{-2}]
$G_{chem,i}$: generation rate by chemical reaction [kg m^{-3} s^{-1}]
$G_{perc,i}$: generation rate by percolative fragmentation [kg m^{-3} s^{-1}]
h_m : mass transport coefficient between gas and particle [m s^{-1}]
k : pre-exponential factor of kinetic constant [kg m^{-2} s^{-1} Pa]
L : reactor height [m]
n_i : particle frequency [s^{-1}]
$P_{j,i}$: size distribution of percolated fragments
P : pressure [Pa]
R_g : gas-law constant [J mol^{-1} K^{-1}]
R_0 : initial percolation rate
R_i : dimensionless percolation rate
S : reactor section [m^2]
T : temperature [K]
U : gas velocity [m s^{-1}]
u_i : particle vertical velocity [m s^{-1}]
w_i, $w_{i,0}$: current, initial mass flow rate [kg s^{-1}]
x_0 : initial carbon content
x_i : carbon content
$Y_{s,i}$: molar fraction of the oxidant species at particle surface
Y_0, Y : initial, current molar fraction of the oxidant species
z : reactor axial coordinate [m]

Greek Letters

γ : reaction order
ε_i, ε_0, ε_{cr} : current, initial and critical particle voidage
λ : gas diffusion exponent
μ : viscosity [Pa s]
ν : exponent of percolation rate
ξ_i : fraction of surface area occupied by carbon
ρ_i : average particle density [kg m^{-3}]
ρ_a : ash density [kg m^{-3}]
ρ_c : carbon density [kg m^{-3}]
$\Phi_{i,0}$: initial particle distribution on mass base
χ : total conversion degree
Ψ : Bhatia and Perlmutter coefficient

REFERENCES

Bhatia, S. K. and Perlmutter, D. D., "A Random Pore Model for Fluid-Solid Reactions: I. Isothermal, Kinetic Control," *AIChE J.*, **26**, 379 (1980).

Chirone, R., Massimilla, L. and Salatino, P., "Comminution of Carbons in Fluidized Bed Combustion," *Prog. Energy Combust. Sci.*, **17**, 297 (1991).

Fuertes, A. B. and Marban, G., "Modelling Gasification Reactions Including the Percolation Phenomenon," *Chem. Eng. Sci.*, **49**, 3813 (1994).

Jung, Y. and Park, D., "Fluidized Bed Combustion of High Ash Anthracite: Analysis of Combustion Efficiency and Particle Size Distribution," *Korean J. Chem. Eng.*, **5**, 109 (1988).

Kang, S., Heble, J. J., Sarofim, A. F. and Beer, J. M., "Time-Resolved Evolution of Fly Ash During Pulverized Coal Combustion," *Proc. of the Combustion Institute*, **22**, 231 (1988).

Kerstein, A. R. and Edwards, B. F., "Percolation Model for Simulation of Char Oxidation and Fragmentation Time-Histories," *Chem. Eng.*

Sci., **42**, 1629 (1987).
Kerstein, A. R. and Niksa, S., "Fragmentation During Carbon Conversion: Prediction and Measurements," *Proc. of the Combustion Institute*, **20**, 941 (1984).
Liu, G., Wu, H., Gupta, R. P., Lucas, J. A., Tate, A. G. and Wall, T. F., "Modeling the Fragmentation of Non-Uniform Porous Char Particles During Pulverized Coal Combustion," *Fuel*, **79**, 627 (2000).
Marban, G. and Fuertes, A. B., "Influence of Percolation on the Modification of Overall Particle Properties During Gasification of Porous Solids," *Chem. Eng. Sci*., **52**, 1 (1997).
Miccio, F. and Salatino, P., "Monte-Carlo Simulation of Combustion-Induced Percolative Fragmentation of Carbons," *Proc. of the Combustion Institute*, **24**, 1145 (1992).
Miccio, F., Moersch, O., Spliethoff, H. and Hein, K. R. G., "Generation and Conversion of Carbonaceous Fine Particles During Bubbling Fluidised Bed Gasification of a Biomass Fuel," *Fuel*, **78**, 1473 (1999).
Mitchell, R. E. and Jacob Akatenuk, A. E., "The Impact of Fragmentation on Char Conversion During Pulverized Coal Combustion," *Proc. of the Combustion Institute*, **26**, 3137 (1996).
Risnes, H., Sørensen, L. H. and Hustad, J. E., "CO_2 Reactivity of Chars from Wheat, Spruce and Coal" in "Developments in Thermochemical Biomass Conversion" (ed. by A. V. Bridgwater), p. 61-72 (2001).
Sahimi, M. and Totsis, T. T., "Dynamic Scaling for the Fragmentation of Reactive Porous Media," *Physical Review Letters*, **59**, 88 (1987).
Salatino, P. and Massimilla, L., "The Role of Percolative Fragmentation in Detachment of Fines from Burning Carbon Particles," *Proc. of the Combustion Institute*, **22**, 29 (1988).
Salatino, P., Miccio, F. and Massimilla, L., "Combustion and Percolative Fragmentation of Carbons," *Combust. and Fl*., **95**, 342 (1993).
Senneca, O., Chirone, R., Salatino, P. and Masi, S., "A Thermogravimetric Study of Nonfossil Solid Fuels. 1. Inert Pyrolysis," *Energy & Fuels*, **16**, 653 (2002).